LABORATORI NAZIONALI DI FRASCATI
SIS – Pubblicazioni

LNF–05/ 19 (P)
October 26, 2005

X-RAY PROPAGATION THROUGH HOLLOW CHANNEL: POLYCAD - A RAY TRACING CODE

Dariush Hampai [1], Sultan B. Dabagov[2,3], Giorgio Cappuccio[1,2]
and Giannantonio Cibin[2,4]

[1]CNR - Istituto per lo Studio dei Materiali Nanostrutturati, I-00016 Montelibretti (RM), Italy
[2]INFN - Laboratori Nazionali di Frascati, I-00044 Frascati (RM), Italy
[3] RAS - P.N. Lebedev Physics Institute, 119991 Moscow, Russia
[3]IMONT, P.za dei Caprettari, 70, I-00186, Rome, Italy

Abstract

"PolyCAD", a CAD program designed for X-ray photon tracing in polycapillary optics, is described. To understand the PolyCAD code and its results, the theoretical bases of X-ray transmission by a single cylindrical channel (monocapillary) are discussed first. Then cases of cylindrical, lens and semi-lens shaped polycapillary optics are examined. PolyCAD allows any type of X-ray source to be used: an X-ray tube of finite beam dimensions or an astrophysical object can be simulated in combination with the polycapillary optics. The radiation density distribution images formed on a screen located at various focal distances are discussed. The good agreement of the PolyCAD results with experimental and previous theoretical findings validate the code.

Published on
Nuclear Inst. and Methods in Physics Research, B journal n. 5212

1 Introduction

The use of polycapillary optics to control X-ray beams in analytical X-ray apparatuses for diffraction and fluorescence analysis is becoming increasingly important. In the near future polycapillary optics will be widely used in many different fields, e.g., aerospace research, medicine, biology, and so on [1]. Our strong interest in the development of these devices led to the idea of creating a ray-tracing program that allows to simulate the process of radiation propagation through polycapillary optical systems and to visualize the radiation distributions at the optical output.

At present there are few procedures available for evaluating X-ray transmission by capillary structures in the case of peculiar configurations, see for instance [2–11]. One of the first papers [2] reported coherent radiation transmission by a hollow glass pipe. This code also considered i) the presence of a rough surface as an X-ray anomalous dispersion effect, ii) radiation penetration into the channel wall, and iii) the possible presence of micro-dust inside the channel.

Another algorithm [3] for X-ray transmission by capillaries of various shapes runs in the geometrical optics approximation; for this reason it is simpler and more flexible than the previous model.

The first X-ray tracing codes were developed in 1992 by [4,5] and by the Institute for Roentgen Optics, for a review look at [12] . However, these simulations used a number of simplifications based either on capillary system with cylindrical symmetry or on the meridional ray approximation, which is valid only for describing radiation propagation through a bundle of channels or a monocapillary concentrator.

To the authors' knowledge, the most advanced and complete softwares for X-ray tracing inside capillary channels are four. The first code [6,9] traces the trajectory of each photon including the corrections of absorption and roughness; according to some experimental results, the authors are able to evaluate the roughness of the channel. The second one [7] uses the SHADOW ray tracing software, adapting it to the channel shape. In addition, recently some new works based on SHADOW ray tracing were published [13, 14]. The last code [8,10] uses a Monte Carlo simulation for X-ray radiation propagation through hollow channels. The theoretical results obtained by this code agree quite well with the experimental data, although the algorithm is rather simple due to the geometrical optics approximation and to the circular cross section of the channel's shape.

The main aim of all these simulation codes is to optimize both the channel size and the optical shape in order to obtain highly efficient optical systems. Obviously, this is very important from the viewpoint of the development of capillary optics technology. However, analysis of the radiation distribution features, reported in a number of papers [15–17] is particularly interesting. (Some of the earlier publications are cited in reference [17]). In these papers the experimental data were validated by means of analytical estimations based on the wave theory of radiation propagation.

Before we continue any further, let us clarify the terminology used in this work: 1) a monocapillary is a single capillary; 2) a polycapillary is a set of closely packed monocapillaries; 3) a lens is a device that concentrate the radiation in a point or in a small region; 4) a semi-lens, or a half-lens is a device that can concentrate a quasi-parallel beam in a point and vice versa by reversing the geometry.

Here, we introduce an X-ray tracing code for polycapillary optics, named *PolyCAD*. A previous version was designed for cylindrical optics only [18,19]. Now, the software can simulate monocapillary and polycapillary optics with any shape. The advantage of the code lies in its precise mathematical solutions for each given optical shape. Comparison of the results of PolyCAD and of the previous algorithms [5–8,12] revealed some differences, due to the fact that PolyCAD is free of many of the algorithmic constraints.

In the first part of our paper the theoretical basis of a cylindrical monocapillary is explained; in the second part numerical results and simulations are reported. In the last part we compare experimental data with our predictions.

2 Theoretical ground

To estimate the correct behavior of the rays inside the capillary, it is possible to use some simple analytical considerations. The total beam intensity $I(\theta)$, where θ is the angle formed by the exit photons direction and the capillary axis, is given by all the contributions of the photon families that pass through the capillary; each family is defined by the number of its reflections:

$$I(\theta) \;=\; I_0(\theta) + I_1(\theta) + \cdots + I_N(\theta) \tag{1}$$

where N is the maximum number of reflections.

It is clear that the intensity $I_m(\theta)$ is strictly dependent on the reflection coefficient R_0, namely, on the m^{th} power of R_0:

$$I_0(\theta) \;=\; R_0 \qquad \theta \in (-\theta_0\,,\,\theta_0) \tag{2}$$

$$\vdots$$

$$I_N(\theta) \;\propto\; R_0^N \qquad \theta \in (-\theta_N\,,\,\theta_N) \tag{3}$$

In order to consider the total radiation intensity on a screen behind a monocapillary,

$I(\theta)$ has to be integrated over the whole plane, so:

$$I_{tot}(\theta) \;=\; \int\int d\phi\, d\theta\, \frac{dI}{d\theta} \;\propto\; \int d\phi \left\{\sum_{i=0}^{N} I_i(\theta)\right\} \;=\; 2\,\pi\, \left\{\sum_{i=0}^{N} I_i(\theta)\right\} \tag{4}$$

the last result is due to the assumption of an axial symmetry of the system.

As can be seen from Fig. 1, if a screen is placed at $P1$, near the focal point $f2$, characterized by the ray family with a maximum number of two reflections, the image on the screen is smaller than in any other configuration. Moreover, for only two reflections, there are five different areas of interaction (Fig. 1). However, if the screen is placed at $P2$, far from the focal point, the picture on the screen does not have a simple shape, but has some zones that are more intense than others (Fig. 1).

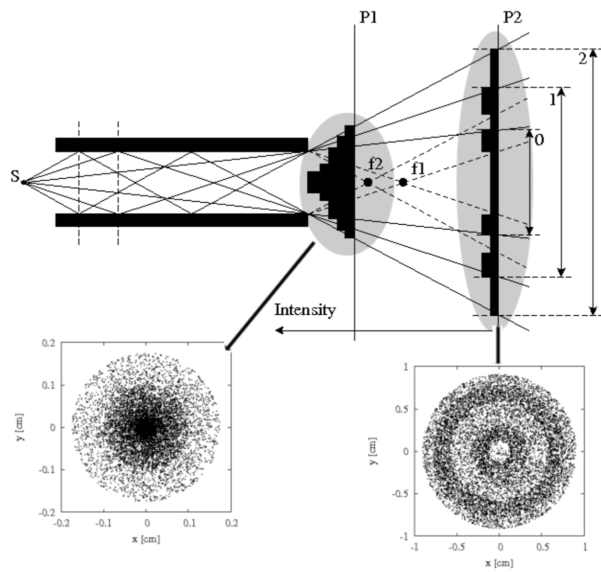

Figure 1: Cross section of the density distribution for a cylindrical monocapillary with on-axis source. The expected beam intensity on the screen located in two different positions is shown. The image shape changes according to the position, please note that areas without any counts are not allowed. Focal points $f1$ and $f2$ are due to rays that undergo one and two reflections, respectively.

The inner surface of the capillary can be divided into a discrete set of zones according to the number (1, 2,...) of reflections of each photon trajectory. If the origin of the reference system (x, y, z) is located at the end of the capillary and the z-axis coincides with the capillary axis, each zone along the surface has a length given by the following expression:

$$z(\theta) \;\simeq\; f \times I(\theta), \qquad (\theta \ll 1) \tag{5}$$

where f is the distance between the end of the capillary and the screen. Looking at Fig. 2 and considering only the upper propagation case, each area has a maximum angle θ and a portion of interaction on the screen, defined by:

$$z_m(\theta) \ \rightarrow \ (-\frac{d}{2} + f\theta_{m-1}, \ \frac{d}{2} + f\theta_m) \qquad R_0^m \tag{6}$$

where d is the diameter of the capillary and R_0^m is the m^{th} reflection coefficient.

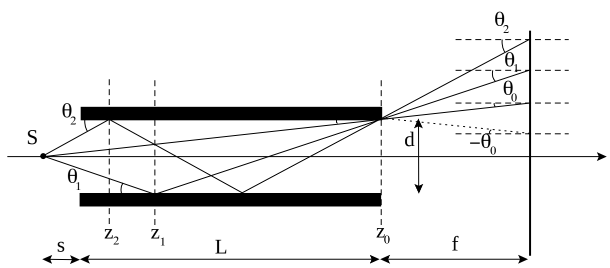

Figure 2: Geometrical description of a cylindrical monocapillary. Length of capillary L; distance from source s; distance from screen f; channel radius d. The maximum exit angle allowed for each ray family is shown. Rays entering between z_0 and z_1 undergo only one reflection, rays between z_1 and z_2 undergo only two, and so on.

The maximum angle for each reflection family can be evaluated as:

$$\theta_m \ = \frac{2m+1}{2} \frac{d}{s+L} \ \Delta\theta_{m,\,m-1} \ = \frac{d}{s+L} \tag{7}$$

From these formulas it is clear that the difference between two consecutive maximum angles is constant and depends only on the properties of the system. When these properties are fixed, the maximum number of reflections can be easily evaluated:

$$\begin{aligned} N \ &= \ \frac{\theta_c - \theta}{\Delta\theta} = \frac{(d/2s) - d/[2(s+L)]}{d/(s+L)} = \\ &= \ \frac{1}{2}\left(\frac{s+L}{s} - 1\right) = \frac{L}{2s} \end{aligned} \tag{8}$$

Since there must be at least one reflection, Eq. 8 becomes the well known expression:

$$N = \left[\frac{L}{2s}\right] + 1 \tag{9}$$

Equation 9 states that the maximum number of reflections depends only on the length and on the diameter of the capillary; this result is exact if the source is placed along the monocapillary z-axis. Equation 9 also remains a good approximation if the source is close to the optical axis (Fig. 1). Obviously, in the general case, there are some problems because an off-axis source makes some zones inside the capillary unsuitable for photon reflection [20] .

3 The code

In our previous report [18] the code was based on the geometrical symmetry of the system, so the radiation image on a screen could be evaluated only if the shape of capillary was cylindrical. We will show here the additional features recently introduced in the PolyCAD code in order to make it more flexible and complete.

During the upgrading of the code in order to include other capillary shapes, the complicated definition of the reflection angle α_{ref} introduced some problems. For a cylindrical capillary it is easy to find the following relation for α_{ref}:

$$\alpha_{ref} = \arccos\left(\frac{\cos\alpha}{\cos\omega}\right) = \arccos\left\{\frac{\cos\alpha}{\cos\left[\arctan\,(\tan\alpha\times\sin\theta)\right]}\right\} \qquad (10)$$

where α is the zenithal angle and θ is the angle on the inlet plane (see Ref. [18]).

Since the *conical polycapillary case*, the ω angle, formed by the two projections of the X photon trajectory and of the z-axis on the tangent plane, is still a function of α and θ, but now there is also an indirect dependence on the conical semi-opening angle β. This indirect dependence is due to the fact that the trajectory of a photon is generally oblique with respect to the capillary axis. Thus, a new parameter that takes into account the off-axis angle must be included, which does not allow us to transfer in a simple way a 3-D problem into a 2-D one, as was done in the case of a cylindrical optics [18]. Nevertheless, by knowing the photon starting point, (i.e., the source point P_s) and the point P_0 on the inlet plane, it is possible to define the vector-direction of the photon. An equation system between the photon path and the capillary surface equation allows to describe the photons trajectory inside any generic capillary optics.

In this paper we will use an elliptical toroid as the shape for full and semi-lens: each channel axis describes an ellipse. The difficulty of describing this optics is due to the fact that the channel is not formed by a complete rotation along the axis like in the case of a circular toroid; in this case we rewrote analytically the surface equations.

4 Numerical results

To show how PolyCAD works we report the most significant results using different source shapes. We will start showing the results obtained using a point source, located at finite or infinite distance, up to a source with a 3-D shape.

4.1 Polycapillary semi-lens

In this section we will consider a polycapillary semi-lens with cylindrical channels. We want to use the optics as a converter of divergent rays to a parallel beam, thus as a preliminary step we considered a point source located at finite distance. The amplitude of the incident angle α can be chosen randomly from zero to any prefixed value according to the distance source-lens: in the optimal set-up each entering ray should be tangent to the channel axis.

The conditions for the simulation are: i) 1 keV and 8 keV point source located at finite distance, ii) semi-lens polycapillary with an inlet radius of 0.8 cm, while the radius of a single channel is $\rho = 0.9\,\mu m$.

In Figs. 3 and 4 the photon density distributions are shown for the two source energy values (1 and 8 keV). The z-axis coincides with the optical system axis. The spatial X photon distribution $n_p\,(x\,,y\,,z)$ is collected by moving the screen xy along z, where n_p is the number of photons per unit area impinging on the screen. The figures 3 and 4 show the distribution $n_p\,(x\,,y=0\,,z)$, i.e. the photon density variation along the optical axis (top image). In the lower panel we report the same density using a contour plot.

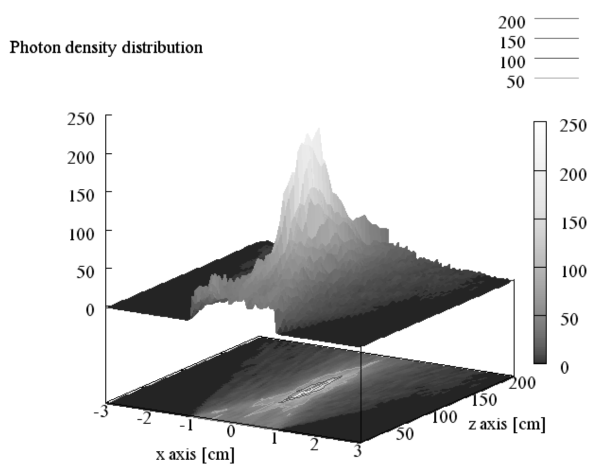

Figure 3: Density distribution for a polycapillary semi-lens along the xz plane with y equal to zero. The calculations were performed in the soft X-ray region (1 keV). Even if the beam is essentially parallel, after ~ 1 meter is evident an increase of the intensity in the central beam region. This effect is due to the residual beam divergence.

Even if the exit beam, in Fig. 3, is not strictly parallel, with simple considerations the density gain can be evaluated by comparing the integrated density distribution in an

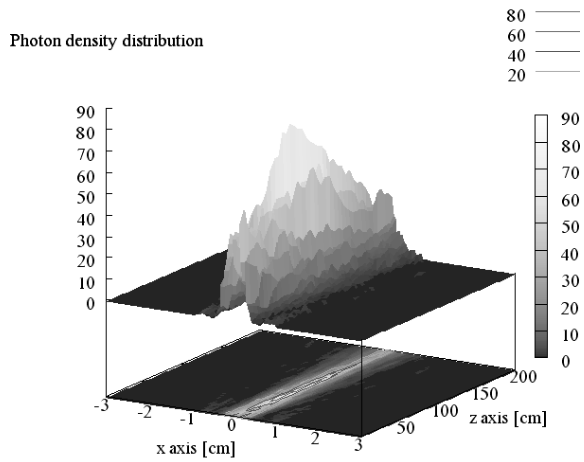

Figure 4: Density distribution for a polycapillary semi-lens along the xz plane with y equal to zero for an 8 keV source. Respect to Fig. 3, the parallel beam behavior is more evident.

area equal to exit optics surface, with and without the insertion of the polycapillary semi-lens. In such a way the density gain measured, e.g. at a distance of 2 meters, is about 100 times.

A polycapillary semi-lens can be used also as a focusing optics for parallel beam. In Figs. 5 and 6 we show the simulation results obtained using a parallel beam source at the same energies and the same polycapillary geometrical parameters as previously used. A sharp intensity peak is formed at a distance from the exit of polycapillary of about 9 cm, showing the presence of a focal point. The size of the focal point area is here defined as the screen area having a beam intensity higher than 10% of the maximum. The gain, i.e. the ratio between the number of photons in the focal point area with and without the lens, is about 17 and 14, respectively, for 1 keV and 8 keV energy sources.

4.2 Evidence of a focusing effect by a cylindrical polycapillary

As a good example of the PolyCAD flexibility in treating different optical configurations we would like to show how a polycapillary optics can manage X-rays coming from a tri-dimensional sources. We will consider two spherical sources located at different positions respect to the cylindrical polycapillary lens (Fig. 7), placed on the y=0 plane.

The cylindrical polycapillary is characterized by the following parameters: i) length 10 cm; ii) polycapillary radius 1 cm, single channel radius $0.9 \cdot 10^{-3}$ cm. The X-ray source is realized by two spherical surfaces emitting isotropically 1 keV photons. The spheres

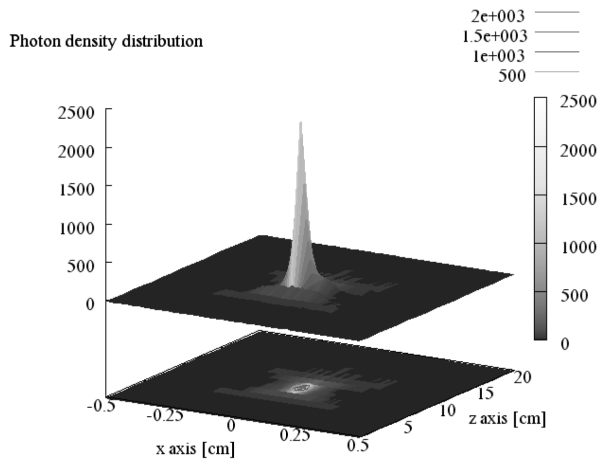

Figure 5: Density distribution (1 keV source) for a polycapillary semi-lens along the xz plane with y equal to zero, in focusing configuration. At the expected distance of about 9 cm, is evident the presence of a focused spot, where the intensity gain is about 17.

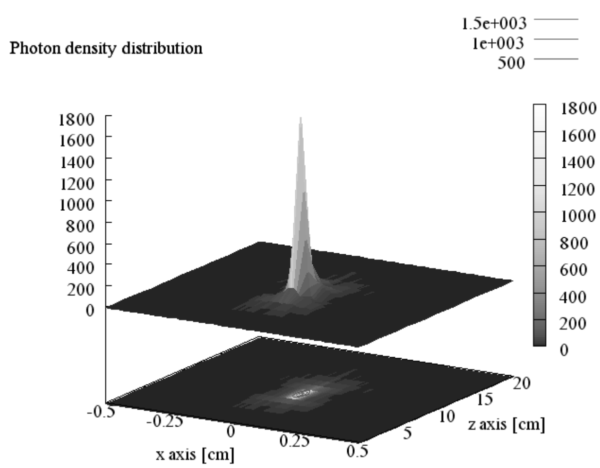

Figure 6: Density distribution (8 keV source) for a semi-lens polycapillary along the xz plane with y equal to zero, in focusing configuration. Like in the previous figure, at the expected distance is evident a focused spot. In this case the gain is about 14.

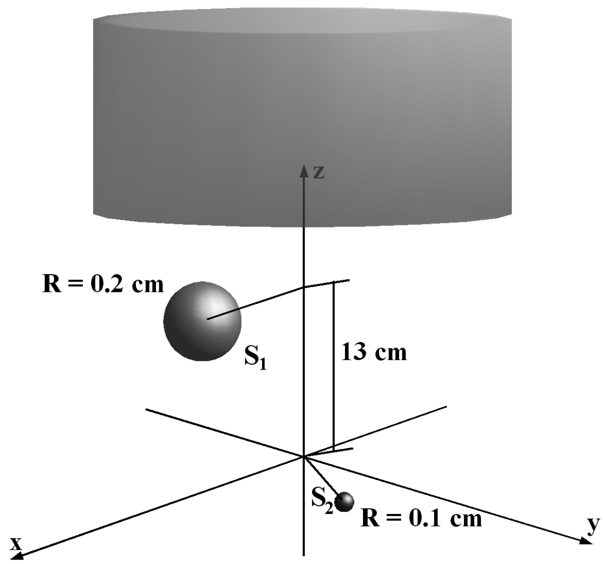

Figure 7: The image shows the position of two source spheres, used for the simulation, respect to the polycapillary optics. The distance of the bigger sphere from the polycapillary inlet plane is about 30 cm.

radius is 0.2 cm (S_1) and 0.1 cm (S_2) respectively. The distance of the bigger sphere from the polycapillary inlet plane is 30 cm, while the distance of the smallest sphere is 43 cm. On the xy plane the spheres distance is 0.56 cm.

In Figs. 8 and 9 are shown the density intensity distributions on the xz plane. As the sphere S_2 is smaller, the intensity peak due to the sphere S_2 is narrower and higher than the one due to the sphere S_1.

Looking at the S_1 focal plane image, there is a significant contribution of S_2 photons, showing that this optical system has a "depth of field" depending on the source distance. Indeed the depth of field seems to be proportionally correlated to the distance of the source.

4.3 Focusing problem with a Full-Lens

As a possible definition of focal plane for a full-lens, and similarly for a semi-lens, we consider the intersection point of the tangent line to the curved channels axis, at the inlet polycapillary surface, with the polycapillary axis. In our calculation we used a lens having entrance and exit focal distances of 8.8 cm.

In Fig. 10 is represented the density distribution on the xz plane, obtained placing a point source along the polycapillary axis in a position having a distance of 5 cm far from

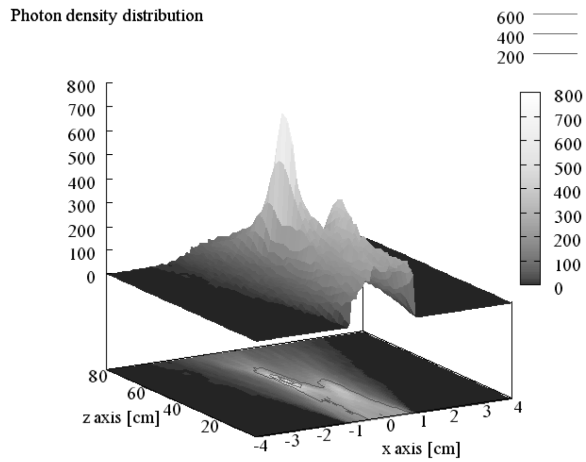

Figure 8: Density distribution along the xz plane with y equal to zero. From the density distribution image it is possible to evaluate the relative distance between the two source spheres.

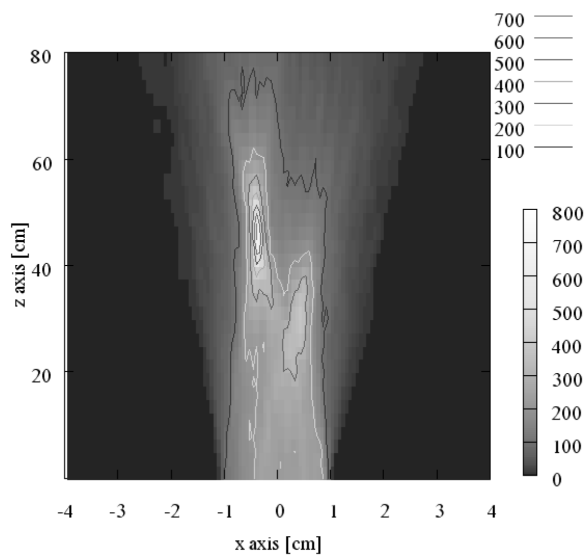

Figure 9: Density distribution on the xz plane. The contour plot highlights the position and shape of the focal points corresponding to the two spherical sources. In particular, a difference in the “depth of field” is evident.

the entrance focal point, using the same polycapillary parameters of the previous section. A first peak is placed symmetrically to the source: nevertheless another peak is present which collects another family of allowed photons, [21,22].

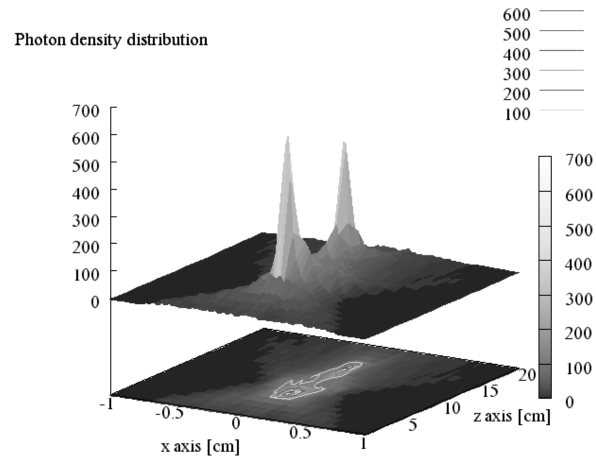

Figure 10: Density distribution along the xz plane with y equal to zero for a polycapillary full-lens. The image shows two peaks, caused by the non-perfect focal positioning of the source; in particular the higher peak is formed by a secondary family of photons, [21,22].

On the contrary, when the source is placed at the correct focal position, as shown in Fig. 11 , a single strong and intense peak is present. Its intensity is about one order of magnitude higher than in Fig. 10. This comparison shows how much can be critical the correct positioning of the lens respect to the source and to the screen, [23–25].

5 Comparison with experimental results

While in our previous work we compared PolyCAD results with theoretical calculations of various authors, [18,19,21,22]; now we can compare PolyCAD with experimental data.

We report the experimental results by Shcherbinin and Dabagov [26], obtained with a polycapillary semi-lens, used at BESSY to focalize synchrotron radiation with an energy of 8 keV. The parameters about this optics are entering and exit diameter 8.5 and 6.3 mm respectively, length ~ 47 mm.

In Fig. 12 we report the density distribution on the xz plane calculated using the same configuration for an elliptical toroid shape. We find a focal spot at about 60 mm, while Shcherbinin and Dabagov reported an experimental focal distance of ~ 74 mm. This discrepancy is due to the fact that we are using an ideal optics, with a perfect elliptical shape having a perfectly regular capillary distribution, without roughness. On the

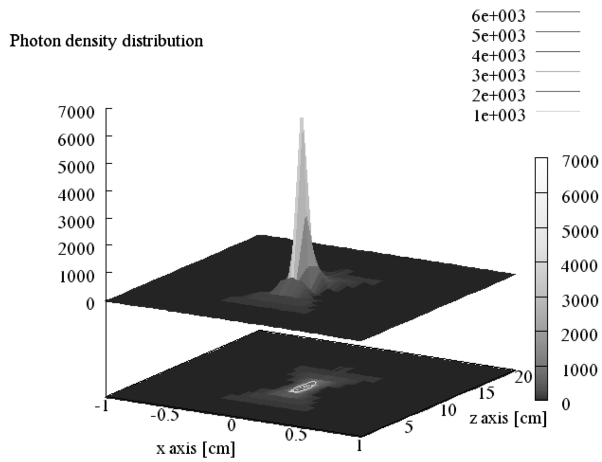

Figure 11: Density distribution along the xz plane with y equal to zero for a polycapillary full-lens. The source is placed in correspondence of the focal point.

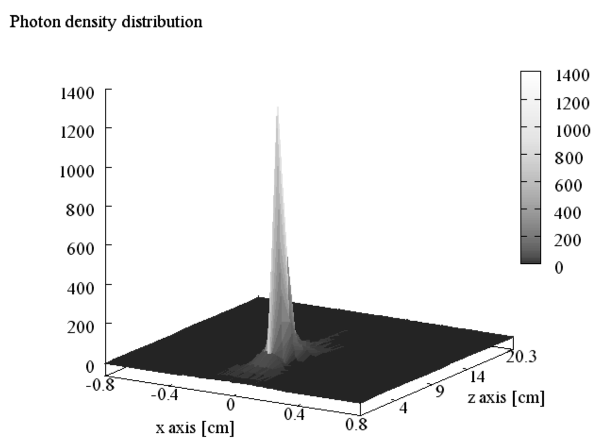

Figure 12: Photon density distribution evaluated on the xz plane for a semi-lens polycapillary.

contrary, as shown on Fig. 13, the spot size at the focal point correspond to the experimental one, about 0.4 mm radius.

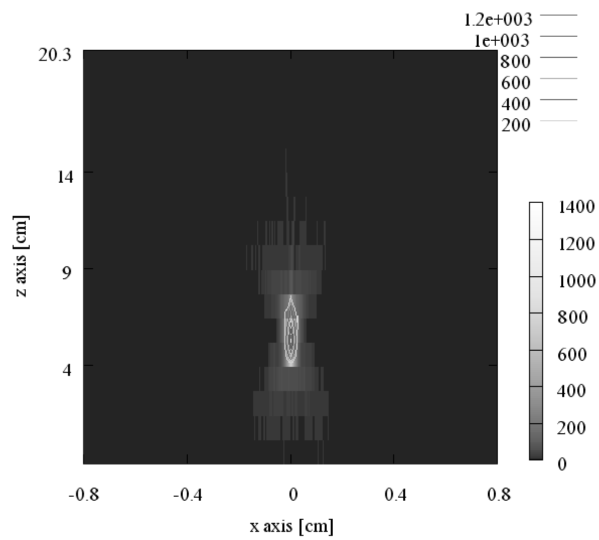

Figure 13: Density distribution on the xz plane. The contour plot highlights the position of the focal points corresponding to a distance of 6 cm far from the polycapillary exit plane.

The quality of our results is emphasized also by our estimation of the transmission coefficient, which is 34% in agreement with the IRO Group result of 39%.

6 Conclusion

In this paper we have reported a description of the *PolyCAD* software designed for polycapillary optics simulations. Using the ray optics approximation in the ideal case of total external reflection, i.e., without absorption effects by the optical channel walls, this algorithm allows us to i) simulate the transport of an X-ray beam inside the capillary channels having different geometrical shapes using point-like or extended sources, ii) analyze the simulation results calculating the photon density distributions and visualizing the spot images formed on screens placed at different positions respect to the optics.

After a description of the theoretical basis and of the computational details, we reported the numerical analysis for various source-optics configurations. This code can accurately describe the radiation distribution behind the optics, as shown in Figs. 5 and 11.

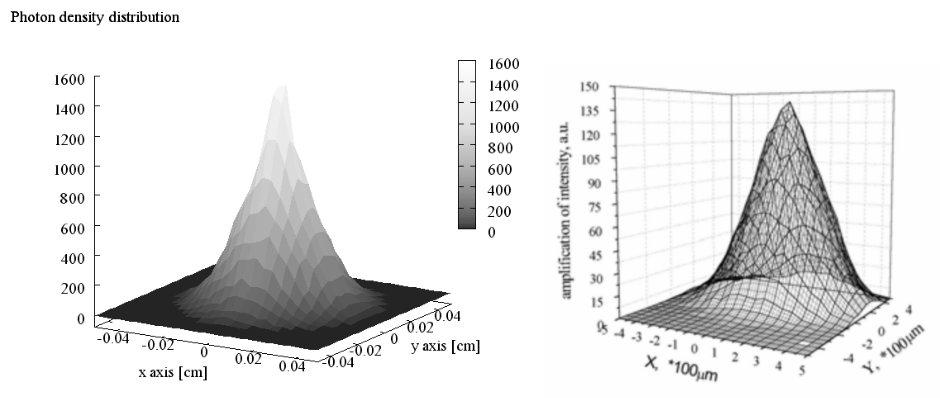

Figure 14: Polycapillary semi-lens photon density distribution on the plane xy when the screen is positioned on the focal point. (Left) Calculation results. (Right) Experimental results [26] obtained using synchrotron radiation source (see text for details). Experimental spot size is estimated as ~ 0.4 mm.

We found a good agreement comparing our theoretical results with experimental data, obtained at BESSY synchrotron radiation. In particular, we obtain a very close value for the transmission coefficient and for the spot dimensions at the focal position. A discrepancy between the focal lengths can be ascribed to the constructive details of the real polycapillary used for the experiment.

At present we are working on improvements of the *PolyCAD* program capabilities to deal with more general polycapillary optics shapes. However, to understand the fine features of X-ray propagation through polycapillary lenses it is mandatory to consider the X-ray wave interaction with the inner capillary surface (see details in the review [17]). This will constitute the future development of *PolyCAD*.

7 Acknowledgment

We are grateful to M.A. Kumakhov for his continuous interest and support. This work was done within the frame of the FSSRIS Project ‘Multipurpose Innovative Plants for the UV and X-ray Production’ (CNR - MIUR, Legge 449/97), and was partly supported by the POLYX project (Group V, LNF - INFN).

References

[1] V.V A.A, Part II, “Application of capillary optics”, in *Selected Papers on Kumakhov Optics and Application 1998-2000*, Proc. of SPIE, Vol. **4155**, 100–150 (2000).

[2] K.Furuta, Y. Nakayama, M. Shoji et al., "Theoretical consideration of intensity of an X-ray microbeam formed by a hollow glass pipe", Rev. Sci. Instr., Vol. **64**, 135–142 (1993).

[3] Chen Baozhen, "A new algorithm for X-ray transmission through a cylinder capillary", Nucl. Instr. Meth., Vol. **B170**, 230–234 (2000).

[4] S.A. Hoffman, D.J. Thiel and D.H. Bilderback, "Developments in tapered monocapillary and polycapillary glass X-ray concentrators", Nucl. Instr. Meth., Vol. **A347**, 384–389 (1994).

[5] D.J. Thiel, "Ray-tracing analysis of capillary concentrators for macromolecular crystallography", J. Synchrotron Rad., Vol. **5**, 820–822 (1998).

[6] Q.F. Xiao, I.Y. Ponomarev, I. Kolomitsev and J.C. Kimball, "Numerical simulations for capillary -based X-ray optics", Proc. SPIE, Vol. **1736**, 227–238 (1992).

[7] G.J. Chen, F. Cerrina, K.F. Voss, K.H. Kim and F.C. Brown, "Ray-tracing of X-ray focusing capillaries", Nucl. Instr. Meth., Vol. **A347**, 407–411 (1994).

[8] L. Vincze, K. Janssens, F. Adams and A. Rindby, "A detailed ray-tracing code for capillary X-ray optics", X-Ray Spectrom., Vol. **24**, 27–37 (1995).

[9] Q.F. Xiao and S.V. Poturaev, "Polycapillary-based X-ray optics", Nucl. Instr. Meth., Vol. **A347**, 376–383 (1994).

[10] P. Engström, A. Rindby and L. Vincze, "Capillary optics", ESRF Newsletter - Instrumentation Reports, 30–31 (July 1996).

[11] L. Vincze, S.V. Kukhlevsky, K. Janssens, "Simulation of poly-capillary lenses for coherent and partially coherent X-rays", SPIE, Vol. **5536**, 81–85 (2004).

[12] *Optics of Beams*, M. A. Kumakhov, (Moscow, IROS, 1994).

[13] A. Liu, "Simulation of X-ray propagation in straight capillary", Math. and Comp. Simul., Vol. **65**, 251–256 (2004).

[14] A. Liu and Y. Lin, "Simulation of X-ray transmission in capillaries with different profiles", Math. and Comp. Simul., Vol. **66**, 577–584 (2004).

[15] S.B. Dabagov and A. Marcelli, “The single reflection regime of X-rays traveling into a monocapillary”, in *Selected Papers on Kumakhov Optics and Application 1998-2000*, Proc. of SPIE, Vol. **4155**, 93–98 (2000); App. Opt., Vol. **38 (36)**, 7494–7497 (1999).

[16] S.B. Dabagov, A. Marcelli, G. Cappuccio and E. Burattini, “On propagation of X-rays in capillary channels”, Nucl. Instr. Meth., Vol. **B187 (2)**, 169–177 (2002).

[17] S.B. Dabagov, “Channeling of neutral particles in micro- and nanocapillaries”, Physics Uspekhi, Vol. **46(10)**, 1053–1075 (2003).

[18] D. Hampai, S.B. Dabagov and G. Cappuccio, “PolyCAD: a new X-ray tracing code for cylindrical polycapillary optics”, LNF-preprint, **LNF-04/03 (IR)** (2004), (http://www.lnf.infn.it/sis/preprint/pdf/LNF-04-3(IR).pdf).

[19] D. Hampai, S.B. Dabagov and G. Cappuccio, “PolyCAD - un programma CAD per ottiche policapillari”, in *n 11 dei Quaderni di Ottica e Fotonica* (2004).

[20] M. A. Kumakhov and F. F. Komarov, “Multiple reflection from surface X-ray optics”, Phys. Rep., Vol. **191(5)**, 289–350 (1990).

[21] D. Hampai, S.B. Dabagov and G. Cappuccio, “PolyCAD: A New X-Ray Tracing Code for Polycapillary Optics”, in *X-Ray and Neutron Capillary Optics*, Proc. of SPIE, in press (2004).

[22] D. Hampai, S.B. Dabagov and G. Cappuccio, “An X-ray tracing code for polycapillary optics”, in *Channeling 2004*, Proc. of SPIE, Vol. **5974** (2004).

[23] G. Cappuccio, S.B. Dabagov and C. Gramaccioni, “Polycapillary condensing lens: alignment procedures and optical performances”, Mat. Sci Forum, Vol. **378-381**, 224–228 (2001).

[24] G. Cappuccio, S.B. Dabagov, C. Gramaccioni and A. Pifferi, “Divergence behavior due to surface channeling in capillary optics”, Appl. Phys. Let., Vol. **78 (19)**, 2822–2824 (2001).

[25] G. Cappuccio and S.B. Dabagov, “Alignment procedure and divergence behavior in capillary optics: first results with X-ray tubes and synchrotron radiation”, Proc. of SPIE, Vol. **4765**, 99–103 (2002).

[26] S. Shcherbinin, W. Leitenberger, A. Erko and S.B. Dabagov, “Polycapillary lens as a condenser of synchrotron radiation”, Bessy Annual Report 2002, 383–384 (2002).